

DRY AND WET ETCHING OF A<sup>III</sup>B<sup>V</sup> MATERIALS FOR  
OPTOELECTRONICS DEVICES

JOZEF BRČKA, ALEKSANDER ŠATKA, JAROSLAVA ŠKRINIAROVÁ, VLADIMIR  
TVAROŽEK and PETER VRONSKÝ

*Microelectronics Department, FEI STU Ilkovičova 3, 81219 Bratislava, Slovakia*

Received 7 April 1995

UDC 538.958

PACS 81.60.Cp

Several A<sup>III</sup>B<sup>V</sup> materials (InP, GaAs, AlGaAs) were etched in a reactive ion etcher using different gas compositions (CH<sub>4</sub>, H<sub>2</sub>, CH<sub>4</sub>+H<sub>2</sub>, BCl<sub>3</sub>, BCl<sub>3</sub>+H<sub>2</sub>). The influence of gas pressure, composition of mixture and RF power were examined. In BCl<sub>3</sub> plasma, etching rate of InP was 10 nm/min, of GaAs about 300 nm/min and of AlGaAs up to 650 nm/min. The increase of the etching rate in BCl<sub>3</sub> and H<sub>2</sub> mixture is caused by a synergistic effect (not only by superposition of etching rates due to a chemical and physical interaction). Etched surfaces were observed by scanning electron microscope. Measurements by secondary ion mass spectrometry were involved into the discussion of the surface contamination. The BCl<sub>3</sub> reactive ion etching process of A<sup>III</sup>B<sup>V</sup> is applicable for deep mesas in optoelectronics devices.

### 1. Introduction

Semiconducting alloys of group III and V elements of the periodic table have properties which make them suitable for special electronic and optical applications. Dry etching offers many advantages over wet etching for device fabrication, including better dimensional control, superior uniformity, compatibility with multichamber processing and less effluents. In view of the increasing complexity of III-V device

vertical heterostructures, dry etching becomes a critical step for device processing.  $A^{III}B^V$  compounds present special processing problems [1]. In particular, the diverse chemistries of the group III and group V elements and the great difference in the physical properties of their compounds with other elements make optimisation of any etching process difficult. Moreover, optimisation is further complicated by the fact that many applications impose unique requirements on the etching process. Generally, major problems encountered in current dry etching of  $A^{III}B^V$  materials are: profile control, surface roughness, surface contamination and surface states. Gas phase diagnostics provided by optical emission spectroscopy can provide real-time information on process stability and reliability. Detection of optical emission from electronically excited states of etch reactants and products can be an effective means to monitor dry etching of  $A^{III}B^V$  heterostructures [2].

## 2. Chlorine- and/or hydrogen-based dry etching

Dry etching of the most common Ga-containing  $A^{III}B^V$  semiconductors (e.g., GaAs, AlGaAs, GaSb) is usually performed with chlorine-based discharges ( $BCl_3$ ,  $CCl_4$  and  $SiCl_4$ ). These gases produce fast etching rates and smooth surface morphologies under most conditions, and the addition of fluorine creates very high selectivities for etching of GaAs over InGaAs or AlGaAs [3]. In the future, the range of gases available for dry etching will be reduced with both  $CCl_4$  and  $CCl_2F_2$  production being effectively eliminated due to their ozone-depleting properties. The use of polymer-forming gases is a problem in high density plasma sources, because of the more complete cracking of the gases and consequent excessive deposition that occurs [4]. Consequently, there is a need to learn as much as possible about the dry etching characteristics of  $A^{III}B^V$  semiconductors in  $BCl_3$  and  $Cl_2$  discharges. Boron trichloride is a particularly attractive discharge, because it getters water vapour and so is quite forgiving of its residual amounts in the vacuum chamber. It also readily attacks the native oxide on  $A^{III}B^V$  materials, and provides smooth, controlled etching. Pure chlorine tends to have extremely fast etching rates and non uniform etching due to the inhibiting native oxide on the semiconductor surface.

It is convenient to think of a plasma etching process as proceeding in five steps [5]: (1) reactant production in the plasma, (2) reactant transport to the surface, (3) reactant adsorption, (4) product formation, and (5) product desorption. The degree to which a particular mechanism is important depends on the discharge operating conditions (i.e., power, frequency, pressure, residence time, electrode material, etc.) as well as on the chemical nature of the reactant gas and substrate.

One of the most important concepts needed to understand plasma-surface chemistry is the synergism of ion and neutral reactions, because it can affect reactant adsorption, product formation and product desorption. Basically, two explanations for ion-enhanced surface chemistry have been proposed [5,6]. First, ion bombardment can stimulate surface reactions, and secondly, ions may stimulate desorption or clean the surface of etch-inhibiting, involatile residues.

Feedstock composition influences the relative importance of each of the five

steps because it affects reactivity, contamination, selectivity, and profile control. In particular, the requirement for volatile product formation has limited the choice of reagents to those containing chlorine, bromine or hydrogen (see Table 1). An appropriate volatility of reaction products at the etched surface are preferable, because high volatility causes a rough surface morphology and involatile surface products prevent etching [7]. Chlorine and chlorinated gases are widely used as the etching gas, but they are corrosive and toxic and the reaction products of chlorine remain on surfaces exposed by the gas. Thus the materials should be heated up to temperatures of 100–300 °C during etching. Recently, also hydrocarbon etching ( $\text{CH}_4/\text{H}_2$ ,  $\text{CH}_4/\text{H}_2/\text{Ar}$ ,  $\text{C}_2\text{H}_6/\text{H}_2$ ) gases have attracted much attention for etching of  $\text{A}^{\text{III}}\text{B}^{\text{V}}$  compound semiconductor [8-13]. Moreover, the hydrocarbon gases have the advantages of nontoxicity and noncorrosiveness. Some typical etch mixtures for  $\text{A}^{\text{III}}\text{B}^{\text{V}}$  materials and process characteristics are shown in Table 2 [14].

TABLE 1.  
Normal boiling point of reactant products of In, Ga, P and As with halogen elements.

Reaction product	Boiling point (°C)	Reaction product	Boiling point (°C)
GaF <sub>3</sub>	1000	AsF <sub>5</sub>	-53
GaCl <sub>2</sub>	535	AsF <sub>3</sub>	-63
GaCl <sub>3</sub>	201	AsCl <sub>3</sub>	130
GaBr <sub>3</sub>	279	AsBr <sub>3</sub>	221
Ga <sub>2</sub> H <sub>6</sub>	139	AsH <sub>3</sub>	-55
InF <sub>3</sub>	>1200	PF <sub>5</sub>	-75
InCl	608	PF <sub>3</sub>	-101
InCl <sub>2</sub>	560	PCl <sub>5</sub>	162
InCl <sub>3</sub>	600	PCl <sub>3</sub>	76
InBr	662	PBr <sub>5</sub>	106
InBr <sub>2</sub>	632	PBr <sub>3</sub>	173
InBr <sub>3</sub>	sub	PH <sub>3</sub>	-88

Technique of a reactive ion etching (RIE) is typically performed at low pressure (1–20 Pa) in a parallel-plate reactor. The discharge is ignited and sustained by application of rf power through a coupling capacitor. Capacitively coupled electrode charges negatively with respect to the body of the plasma and space-charge region (sheath) is formed between them. The sample placed on this powered electrode is subject to intense ion bombardment. This process is shown schematically in Fig. 1. The electrons are heated by the applied rf field and have typical temperatures of  $\approx 10$  eV. Neutral and ion temperature is usually  $< 1$  eV. RIE has an advantage of synergism between physical and chemical etching mechanisms and is able to provide fast anisotropic etching.

TABLE 2.  
Typical etch mixtures for  $A^{III}B^V$  semiconductors [14].

Chemistry	Comments	Typical rates
Cl <sub>2</sub> -based Cl <sub>2</sub> , SiCl <sub>4</sub> , BCl <sub>3</sub> , CCl <sub>2</sub> F <sub>2</sub>	Usually have additions of Ar or He. Smooth for GaAs, rough for InP.	300 nm/min for GaAs, 30 nm/min for InP.
CH <sub>4</sub> /H <sub>2</sub> based CH <sub>4</sub> /H <sub>2</sub> , C <sub>2</sub> H <sub>6</sub> /H <sub>2</sub> , C <sub>3</sub> H <sub>8</sub> /H <sub>2</sub> , CH <sub>4</sub> /He	Ar often added for stability smooth etching of InP Heavy polymer deposition.	30 nm/min for InP and InGaAs, lower for GaAs.
I <sub>2</sub> -based HI, CH <sub>3</sub> I, C <sub>2</sub> H <sub>5</sub> I, I <sub>2</sub>	High rates at room temperature InP. Corrosive. No polymer deposition	500 nm/min for InP and InGaAs, 300 nm/min for GaAs.
Br <sub>2</sub> -based HBr, CF <sub>3</sub> Br, Br <sub>2</sub>	Corrosive.	60 nm/min for GaAs, 40 nm/min for InP.

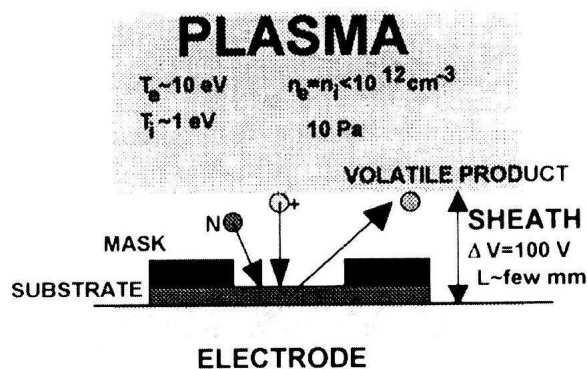


Fig. 1. Schematic representation of the reactive ion etching process.

### 3. Experiment

The experiments were carried out in the RIE chamber of PDS 520/530 (Vacutec AB), which is a conventional type with parallel electrodes and an RF generator at 13.56 MHz. We used BCl<sub>3</sub> (3.0, UCAR), CH<sub>4</sub> (3.5, Messer Griesheim GmbH, Duisburg) and their mixture with H<sub>2</sub> (Linde) as the etching gases. Samples of InP, GaAs and GaAs with 600 nm AlGaAs layer were coated by 1–5  $\mu\text{m}$  positive photoresist SCR-15. They were etched without an intentional heating during the RIE process. The etched-off steps were measured on Talysurf (Rank Taylor Hobson). Morphology of the etched surfaces was observed by the scanning electron microscope BS-300 with automated acquisition of data and numerical processing of the pictures. Optical spectra were measured by the measuring system PSS-3A (Ben-

tham). System consists of a symmetrical Czerny-Turner monochromator with 300 mm focal length and equipped with a 1800 grooves/mm grating. The resolution is 0.5 nm and the available spectral range is 185–650 nm using the detector EMI 9781B. The spectrometer is connected to a view port of the RIE chamber.

#### 4. Results and discussion

Dry and/or wet etching is used for mesa shaping of the vertical structure optoelectronic and microwave devices. Major advantage of the wet chemical etching is a very low surface roughness, usually well defined etching rate and a relative good

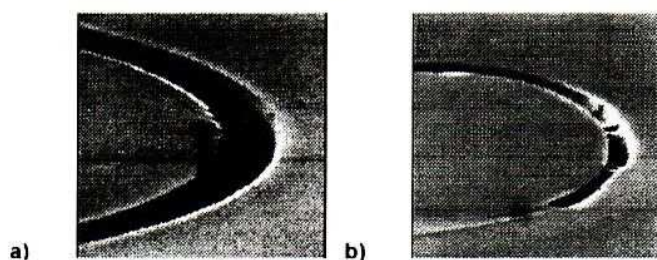


Fig. 2. Scanning electron micrographs of the mesa etches in InGaP/GaAs: (a) shallow (200 nm), (b) overetched with nonuniform and deep pattern in substrate material.

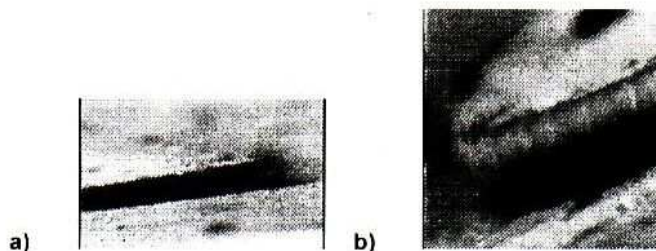


Fig. 3. Wet undercutting of 500 nm thick gold masking layer on AlGaAs/GaAs HBT structure (a) and (b) is detail of edge of the gold layer.

control of homogeneous materials. As an example, the mesa shaped InGaP layer with etch depth of 200 nm is shown in Fig. 2a. Different etching rate of etchants for various materials can be responsible for an undesirable results. For example, etchant  $\text{HCl}:\text{H}_3\text{PO}_4:\text{H}_2\text{O}_2$  (1:10:1) has approximately 50 times higher etching rate in GaAs substrate in comparison to the InGaP (rate of 510 nm/min to 25 nm/min at 20 °C, respectively). When thickness of InGaP is slightly nonuniform, it can result in undefined etching profile and etch depth (see Fig. 2b). Another, but important problem in application of wet etching is underetching of the masking or

other functional layers of different composition. Illustration of under-etched gold layer on AlGaAs/GaAs HBT structure is shown in Fig. 3.

#### 4.1. GaAs and AlGaAs etching in $\text{BCl}_3$ plasma

GaAs substrates were etched in  $\text{BCl}_3$  plasma at pressures in the range from 3 Pa to 20 Pa, flow rate 30 sccm and RF power 225 W. The dependence of etching rate on  $\text{BCl}_3$  pressure is shown on Fig. 4. Etched surface of sample was rough (Fig. 5a). The facets were observed on the top of profile (Figs. 5b and 5c). The facets were more evident at lower pressure, when a pure ion sputtering could be assumed as dominant etching mechanism (Figs. 5b and 5d). Thus, facets can be explained by angle dependent sputtering rate of GaAs and by intense erosion of the resist walls (schematically shown in Fig. 6). The profile had vertical walls (anisotropically etched) with no undercutting (Fig. 5e and 5f).

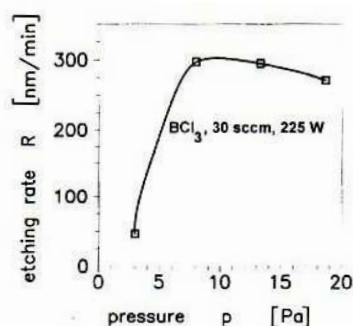


Fig. 4. Dependence of etching rate of GaAs on  $\text{BCl}_3$  pressure.

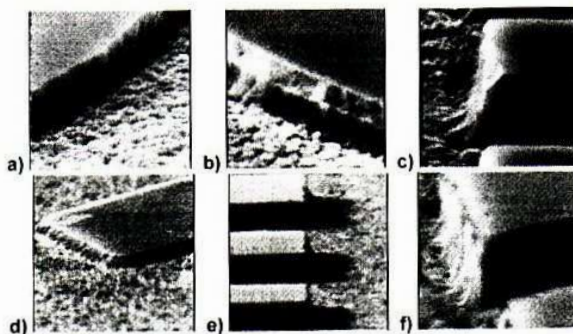


Fig. 5. Scanning electron micrographs of GaAs after reactive ion etching for 10 minutes in a  $\text{BCl}_3$  plasma (RF power 225 W, gas flow rate 30 sccm): a) and c) are micrographs of GaAs surfaces etched at 18.7 Pa (step height is  $2.7 \mu\text{m}$ ), b) and d) at 8 Pa (step height is  $2.97 \mu\text{m}$ ), e) and f) at 13.3 Pa (step height is  $2.95 \mu\text{m}$ ).

The GaAs substrates with AlGaAs layers (600 nm) were etched in a  $\text{BCl}_3$  plasma. Dependence of the etched depth on time is shown in Fig. 7. Etched surface was rough (Fig. 8a), sidewalls of profile were nearly vertical ones (Fig. 8b). The interface between AlGaAs and GaAs could be observed on etched profile (Fig. 8c).

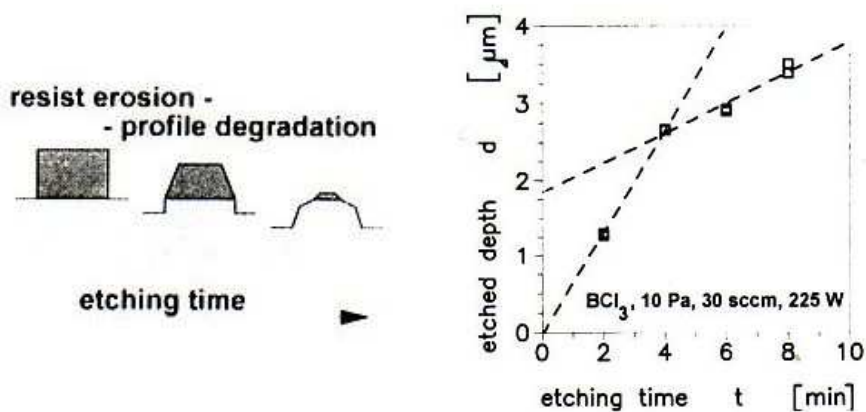


Fig. 6. Degradation of the profile as a result of resist erosion.

Fig. 7. The dependence etched depth on time dependence at RF power 225 W, 30 sccm of  $\text{BCl}_3$  and pressure 10 Pa (right).

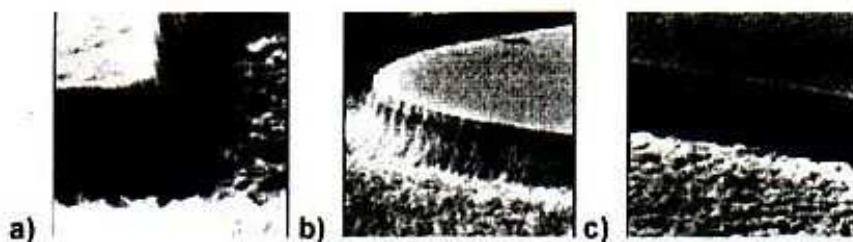


Fig. 8. Scanning electron micrographs of AlGaAs/GaAs after reactive ion etching in a  $\text{BCl}_3$  plasma (10 Pa, 225 W, 30 sccm): a) and c) after etching for 8 minutes (height of step is  $3.45 \mu\text{m}$ ), b) after 4 minutes (height of step is  $2.66 \mu\text{m}$ ).

#### 4.2. InP etching

*Etching in the  $\text{CH}_4$  plasma* (6 Pa, 20 sccm, 250 W): Operating conditions were the following:  $\text{CH}_4$  pressure was 6 Pa, flow rate 20 sccm, and the RF power was 250 W ( $0.4 \text{ W/cm}^2$ ). The process was characterized by strong erosion of the photoresist. The further problem was unremovable residua from photoresist or polymerized from methane plasma, which could not be removed neither in an oxygen plasma nor in an acetone bath.

*Etching in the H<sub>2</sub> plasma* (6 Pa, 30 sccm, 250 W): To maintain the stable discharge, it was necessary to apply, at first, the exciting power to the mixture of the methane and hydrogen (for several seconds), and afterwards the flow of the methane was reduced. No erosion of the photoresist was observed in 30 minutes of exposure. However, the etching rate was very low, about 2 nm/min. The etching at increased pressure of the hydrogen ( $\geq 12$  Pa) was abrupt. The application of a Hg-Xe lamp (400 W) built in the upper part of chamber (behind the electrode) has a consequence of increasing the etching rate up to 2.8 nm/min. The surface of InP substrate was heavily eroded.

*Etching in the mixture of CH<sub>4</sub>+H<sub>2</sub> plasma* (6 Pa, 250 W): In these experiments the flow of methane was varied from 0 to 30 sccm, while the flow rate of hydrogen was kept at constant value (30 sccm). The dependence of etching rate on the ratio CH<sub>4</sub>:(CH<sub>4</sub>+H<sub>2</sub>) is given in Fig. 9. The increase of the etching rate with increasing amount of methane in the mixture (up to 40 %) was observed. At higher ratios a polymerization of the InP surface have occurred. Also, higher degradation of resist and InP surface was evident. In Ref. 15 the carbon atoms bound to indium have been revealed in CH<sub>4</sub>/H<sub>2</sub> RIE-etched surfaces by X-ray photoelectron microscopy (XPS) measurements. The etching damage induced by RIE processing also in the mixture of another hydrocarbon gas with hydrogen (C<sub>2</sub>H<sub>6</sub>/H<sub>2</sub>) was reported [7]. Application of Hg-Xe lamp in our conditions, or increasing of pressure has no effect on the etching rate. The same results were obtained also for InP doped by Sn.

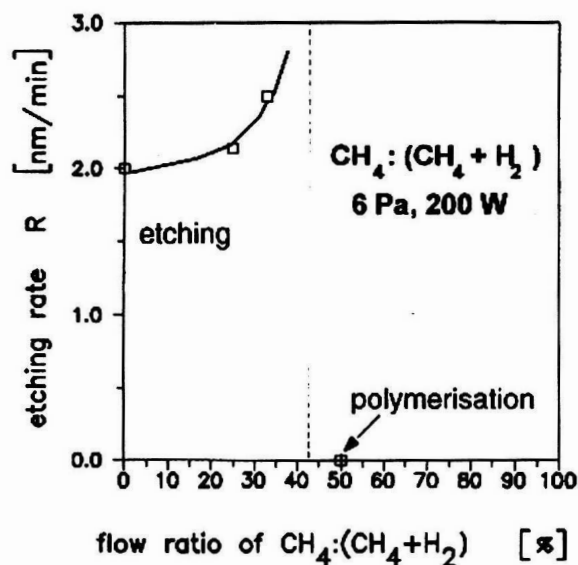


Fig. 9. Etching rate vs. ratio  $\text{CH}_4:(\text{CH}_4+\text{H}_2)$ .

*Etching in the BCl<sub>3</sub> plasma:* The dependence of etching rate on pressure of BCl<sub>3</sub> gas is illustrated in Fig. 10a. In this case higher etching rates were observed (up to



12 nm/min). Etched profile was anisotropic, surface of InP was moderately waved. At pressures higher than 20 Pa, a thin polymer layer on InP surface appeared. The etching rate strongly increased with higher RF power. Its value reached values up to 33 nm/min (see Fig. 10b).

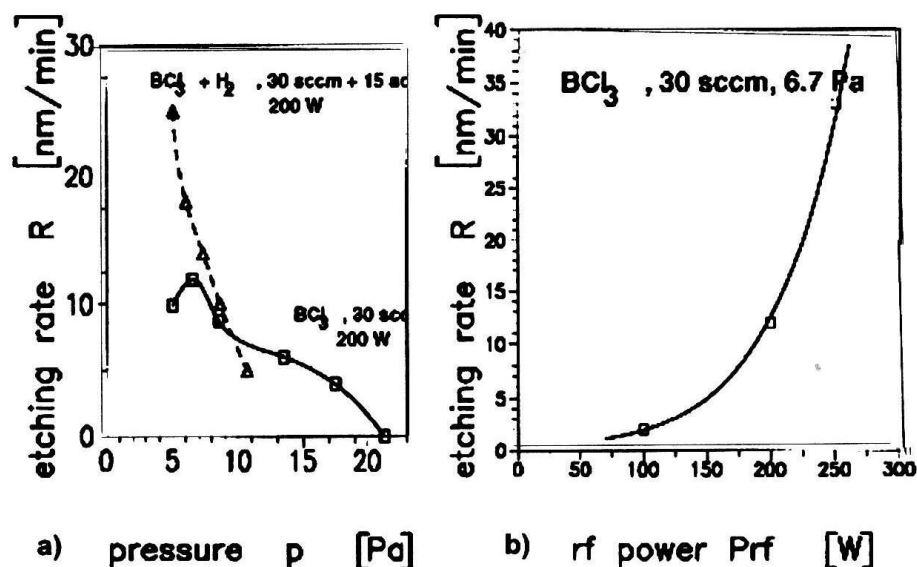


Fig. 10. a) Etching rate vs. pressure in  $\text{BCl}_3$  and  $\text{BCl}_3 + \text{H}_2$  plasma. b) Etching rate vs. RF power in  $\text{BCl}_3$  plasma.

*Etching in the  $\text{BCl}_3 + \text{H}_2$  plasma (30+15 sccm, 200 W):* The addition of hydrogen had the effect of further increasing of the etching rate (see Fig. 7). In comparison to the results in Fig. 10a, the etching rate was three times higher than in pure  $\text{BCl}_3$ , especially in low pressure region. The etched profile was anisotropic, and the surface smooth.

#### 4.3. OES and SIMS analysis

The ratio of several optical emission spectra of  $\text{CH}_4 - \text{H}_2$  based mixture in range from 200 to 700 nm are shown in Fig. 11. The CH radical emission peak at 431.4 nm was detected in plasma. There is no significant difference in optical spectra of  $\text{CH}_4$  plasma in range 6–12 Pa (Figs. 11a and b). When hydrogen is added into mixture the discharge is getting more  $\text{H}_2$ -like (Figs. 11c, d and e) and  $\text{CH}_x$  radicals are polymerized on the surface. The surface of InP with unknown polymerized film was analysed by SIMS method. The analysis shows that clusters of  $\text{C}_n\text{H}_m$  or  $\text{C}_n\text{H}_m\text{O}$ , were on the surface where the number  $n$  is larger than 3. The surface of InP exposed to atmosphere had only clusters with  $n \leq 3$ . After 30 min sputtering of InP surface, the analysis was repeated, and the clusters were not observed.

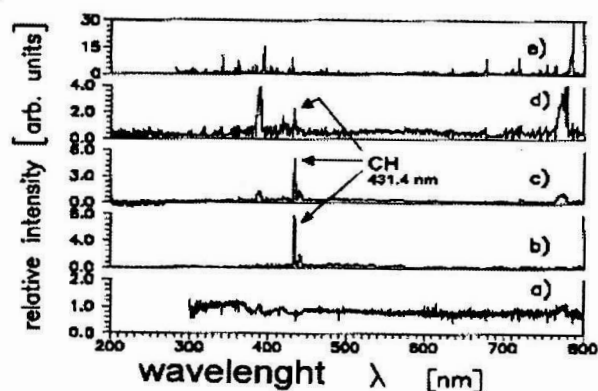


Fig. 11. Ratio of spectra for a)  $\text{CH}_4$  at 12 Pa to  $\text{CH}_4$  at 6 Pa, b)  $\text{CH}_4$  at 6 Pa, c)  $\text{H}_2+\text{CH}_4$  (1:2) to  $\text{H}_2$ , d)  $\text{H}_2+\text{CH}_4$  (2:1) to  $\text{H}_2$ , e)  $\text{H}_2$  to Ar.

## 5. Conclusions

The reactive ion etching of InP semiconductor substrates was investigated using various working gases ( $\text{CH}_4$ ,  $\text{H}_2$ ,  $\text{BCl}_3$ ) and their mixtures. The influence of gas pressure, mixture composition and RF power (in the case of  $\text{BCl}_3$  gas) were examined. Also, the influence of InP substrate type was studied. The samples doped with Sn exhibited lower etching rate (or no etching), probably due to the passivation of dopants by hydrogen. The maximal etching rate was observed in the mixture  $\text{BCl}_3+\text{H}_2$ . The increase of the etching rate in  $\text{BCl}_3$  and  $\text{H}_2$  mixture could be caused by a synergistic effect (not only by superposition of etching rates due to a chemical and physical interaction). The surface was smooth. In our opinion, the reason for that is a rather lower etching rate. Etched profile was anisotropic. The results of an optical emission spectroscopy of reactive plasma and SIMS measurements induced a discussion of the InP etching behaviour. In the carbon-hydrogen mixture, the CH-compound rich plasma has been produced, which has as a consequence the creation of  $\text{C}_n\text{H}_m$  or  $\text{C}_n\text{H}_m\text{O}$  clusters on the InP surface. The use of  $\text{CH}_4/\text{H}_2$ , for etching of deep mesas (several micrometers) in InP is not practical because of low etching rates. Using of  $\text{BCl}_3$  discharge provides reasonable etching rates both for InP and more for GaAs (or AlGaAs/GaAs).

### Acknowledgement

This work was supported by national Grant Agency for Science (N<sup>o</sup>1752/94 and N1738/94). We also wish to thank J. Kocanda for results by SIMS and J. Jakabovič for lithography.

## References

- 1) R. H. Burton, R. A. Gottscho, and G. Smolinsky: *Dry Etching of Group III-group V Compound Semiconductors* (chapt. 3 in: *Dry Etching for Microelectronics*, ed. by Powell, R.A.) North-Holland Physics Publishing Amsterdam (1984);
- 2) K. L. Seaward, N. J. Moll, D. J. Coulman and W. F. Stickle, *J. Appl. Phys.* **61** (1987) 2358;
- 3) S. J. Pearton, M. J. Vasile, K. S. Jones, K. T. Short, E. Lane, T. R. Fullowan, A. E. von Neida and N. M. Haegl, *J. Appl. Phys.* **65** (1989) 1281;
- 4) S. J. Pearton, U. K. Chakrabarti, A. Katz, A.P. Perley, W. S. Hobson and M. Geva: *Plasma Chem. Plasma Proc.* **11** (1991) 405;
- 5) J. W. Coburn, and H. F. Winters, *J. Vac. Sci. Technol.* **16** (1979) 391;
- 6) V.M. Donnelly, D. L. Flamm and D. E. Ibbotson: *J. Vac. Sci. Technol.* **A1** (1983) 626;
- 7) K. Ohtsuka, T. Ohishi, Y. Abe, H. Sugimoto and T. Matsui, *J. Appl. Phys.* **70** (4) (1991) 2361;
- 8) U. Niggerbeugee, M. Klug and G. Garus, *Inst. Phys. Conf. Ser.* **79** (1985) 367;
- 9) N. Vodjdani and P. Parrens, *J. Vac. Sci. Technol. B* **5** (1987) 1591
- 10) T. R. Hayes, M. A. Dreisbach, P. M. Thomas, W. C. Dautremont-Smith and L. A. Heimbrook, *Appl. Phys. Lett.* **55** (1989) 56;
- 11) T. Matsui, H. Sugimoto, T. Ohishi and H. Ogata, *Electron. Lett.* **24** (1988) 798;
- 12) T. Matsui, H. Sugimoto, T. Ohishi, Y. Abe, K. Ohtshuka and H. Ogata, *Appl. Phys. Lett.* **54** (13) (1989) 1193-1194.
- 13) P. Collot, T. Diallo and J. Canteloup, *J. Vac. Sci. Technol.* **B9(5)** (1991) 2497;
- 14) S. J. Pearton: *ECR High Ion Density Plasma Sources for Etching and Deposition in III-V Semiconductor Device Technology*, Society of Vacuum Coaters: 37th Annual Technical Conference Proceedings (1994);
- 15) T. R. Hayes, U. K. Chakrabarti, F. A. Baiocchi, A. B. Emerson, H. S. Luftman and W. C. Dautremont-Smith, *J. Appl. Phys.* **68** (1990) 785.

SUHO I MOKRO JETKANJE A<sup>III</sup>B<sup>V</sup> MATERIJALA ZA  
OPTOELEKTRONIČKE NAPRAVE

Nekoliko A<sup>III</sup>B<sup>V</sup> materijala (InP, GaAs, AlGaAs) su reaktivno ionski jetkani različitim plinskim smjesama (CH<sub>4</sub>, H<sub>2</sub>, CH<sub>4</sub>+H<sub>2</sub>, BCl<sub>3</sub>, BCl<sub>3</sub>+H<sub>2</sub>). U BCl<sub>3</sub> plazmi brzina jetkanja InP bila je 10 nm/min, GaAs oko 300 nm/min, a AlGaAs do 650 nm/min. Jetkane su površine proučavane skanirajućim elektronskim mikroskopom. Reaktivno ionsko jetkanje u BCl<sub>3</sub> može se primijeniti za duboke utore optoelektroničkih naprava.